INSTITUTE OF PHYSICS PUBLISHING SUPERCONDUCTOR SCIENCE AND TECHNOLOGY

Supercond. Sci. Technol. **18** (2005) 1168–1175 doi:10.1088/0953-2048/18/9/004

Pulsed electron deposition of fluorine-based precursors for $YBa_2Cu_3O_{7-x}$-coated conductors

H M Christen[1,4], D F Lee[2], F A List[2], S W Cook[2], K J Leonard[2], L Heatherly[2], P M Martin[2], M Paranthaman[3], A Goyal[2] and C M Rouleau[1]

[1] Condensed Matter Sciences Division, Oak Ridge National Laboratory, Oak Ridge, TN 37831-6056, USA
[2] Metals and Ceramics Division, Oak Ridge National Laboratory, Oak Ridge, TN 37831, USA
[3] Chemical Sciences Division, Oak Ridge National Laboratory, Oak Ridge, TN 37831, USA

E-mail: christenhm@ornl.gov

Received 18 April 2005
Published 25 July 2005
Online at stacks.iop.org/SUST/18/1168

Abstract
Pulsed electron deposition (PED), an ablation-based film growth technique similar to pulsed-laser deposition, is a relatively new method for the physical vapour deposition (PVD) of thin films. This paper describes the implementation of PED in a reel-to-reel apparatus for the room-temperature deposition of fluorine-based precursors onto buffered and textured Ni–W tapes (RABiTS). These precursors have been converted into superconducting $YBa_2Cu_3O_{7-x}$ films with high critical currents. The influence of the PED parameters, the background gas pressure, and the target composition on the resulting material is analysed. Ion-probe measurements are used to monitor the deposition process and aid in the determination of the optimum deposition conditions. Special emphasis is placed on issues related to throughput and reliability. The strengths of the PED approach are discussed together with a careful analysis of the open issues and limiting factors that determine whether this method can be used for the commercial fabrication of coated conductors.

1. Introduction

The widespread use of complex oxides in large-scale applications necessitates efficient, reliable, and economic processes for the deposition of multi-component materials. Pulsed electron deposition (PED), an ablation-based film growth technique similar to pulsed-laser deposition but based on much simpler equipment, is a comparatively new method for such applications. In this paper, results are presented that demonstrate the potential of PED for the large-scale production of superconducting tapes via an *ex situ* process (i.e. a method where a fluorine-based precursor is first deposited and then converted into $YBa_2Cu_3O_{7-x}$ in a subsequent thermal treatment). We illustrate how a careful choice of parameters yields a reliable and reproducible approach, and show how *in situ* diagnostics based on ion-probe measurements can serve as an efficient method to optimize and control the process. This paper focuses primarily on the technical aspects of the deposition method; results for superconducting tapes are shown as a general illustration, with more details being described elsewhere [1].

The basic ideas of using a pulsed electron beam for the ablation of material from a solid target and the deposition of multi-component thin films were developed shortly after the introduction of pulsed laser deposition, and the first applications of PED included the growth of ZrO_2 [2] and $YBa_2Cu_3O_{7-x}$ [3, 4], using a pseudo-spark process to generate electrons from a hollow cathode. In this method, magnetically self-pinched electrons are accelerated through a stack of

[4] Author to whom any correspondence should be addressed.

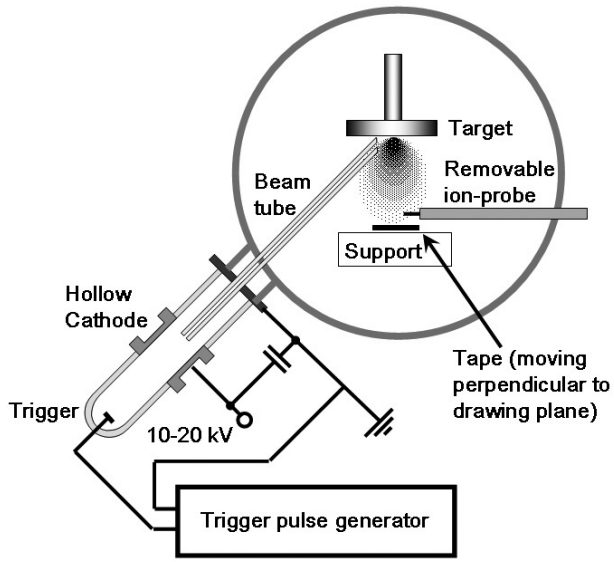

Figure 1. Schematic representation of the pulsed electron deposition apparatus.

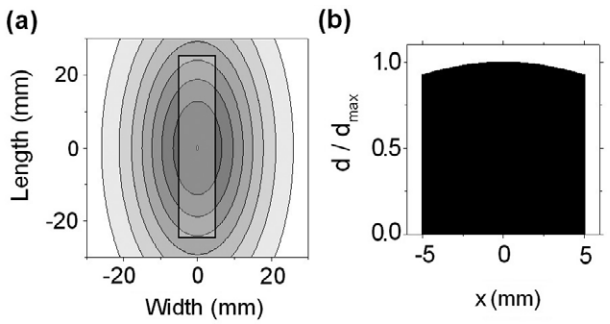

Figure 2. (a) Spatial variation of the deposited material, determined from profilometry and a fit to Gaussian profiles. The rectangular outline at the centre (1 cm × 5 cm) corresponds to the aperture through which the deposition occurs. (b) Lateral thickness profile resulting from the deposition onto a tape moving vertically through the rectangular deposition zone as illustrated in (a).

insulating and metallic rings, while in the subsequently developed channel-spark approach [5, 6], narrow insulating pipes are used for electron acceleration. A commercial PED source is now available from Neocera, Inc. (Beltsville, MD), and recent work has focused on understanding the pulse parameters and ablation mechanisms [7] and on the application to other materials, such as transparent conducting oxides [8]. In our own previous work [9], epitaxial films of $YBa_2Cu_3O_{7-x}$ were grown directly on buffered, textured Ni–W tapes (RABiTS), reaching values of $J_c \approx 1.6$ MA cm^{-2} on short lengths. A more complete review of the PED technique is found in [10].

For the current work, PED was used for the room-temperature, reel-to-reel deposition of fluorine-based precursors onto textured and buffered Ni–W RABiTS tapes. This approach for the fabrication of coated conductor tapes differs significantly from the numerous *in situ* methods (where $YBa_2Cu_3O_{7-x}$ is grown directly at an elevated substrate temperature, such as pulsed laser deposition (PLD) [11–15], metalorganic chemical vapour deposition (MOCVD) [16], thermal co-evaporation [17] and dc sputtering [18]). *Ex situ* processes, such as those using solution-based metalorganic decomposition (MOD) precursors [19, 20] and e-beam co-evaporated, BaF_2-based precursors [21–23], separate the precursor deposition step from the YBCO epitaxial growth process. Advantages of this approach include the usage of a reactor furnace where temperature control during YBCO formation is simplified, and the possibility of a large conversion volume for enhanced production throughput. MOD is generally considered a cost-effective method for precursor deposition; however, the consistent deposition of crack-free, thick (>2 μm) precursors in long lengths appears to be difficult to achieve. On the other hand, very thick (>5 μm), dense, and crack-free precursor films can be deposited by electron-beam co-evaporation.

Electron-beam evaporation techniques require a high vacuum environment and thus elaborate differential pumping if the deposition is to occur in a background gas. Furthermore, with the exception of a recently introduced approach where powders of complex oxides are continuously fed onto and evaporated from a rotating copper plate [24], each element to be deposited requires an independently controlled source, making the addition of dopants or the alloying between multiple complex compounds rather cumbersome. In contrast, PED uses a single, solid source of the mixed starting material, yet relies on equipment that is much simpler than the comparatively expensive excimer lasers [25] used in PLD—an approach that would otherwise offer the same advantages.

The structure of this paper is as follows. First, we describe the apparatus and its overall characteristics, focusing on stoichiometry control and high deposition rates. The use of an ion probe yields information about the energetics and stability of the process. Issues specific to the precursor deposition for $YBa_2Cu_3O_{7-x}$-coated conductors are then discussed, followed by an analysis of the requirements for potential industrial applications of this method.

2. Deposition apparatus and precursor targets

For the work presented here, a commercially available PED source (Neocera, Inc., Beltsville, MD) was integrated with a reel-to-reel apparatus for the room-temperature deposition onto continuously moving tapes, as shown schematically in figure 1. The pulsed electron source is flange-mounted onto the vacuum chamber, and the electrons are guided to the target via a 6.35 mm outer diameter/4.75 mm inner diameter alumina tube. The end of the beam tube is positioned within 2–3 mm from the target surface. A typical pulse carries a current of ~1000 A, with a pulse duration of ~100 ns.

The tape to be coated travels between two reels in a reciprocating action—multiple passes are performed for a full deposition, with the tape travelling at a fixed speed of about 5 m h^{-1}.

Figure 2(a) shows the spatial distribution of ablated material in the plane of the travelling substrate. The plot shows a calculated profile given as a product of a Gaussian variation in the horizontal direction and a Gaussian variation in the vertical direction, with the parameters determined from

a least-square fit to 15 data points obtained by profilometry. The width of the profile is a function of the target-to-substrate distance, which must be chosen as a compromise between two opposite constraints: a short target-to-substrate distance yields a higher collection efficiency of the ablated material, but also a larger thickness non-uniformity. For a tape travelling through a 5 cm long deposition zone (as schematically indicated in figure 2(a)), the resulting thickness profile across a 1 cm wide tape is shown in figure 2(b). The thickness profile along the length of the tape is highly uniform due to the averaging effects of the multiple-pass tape motion.

According to the profile in figure 2(a), 25% of the deposited material is deposited onto the tape. Actual experiments (thickness measurements on long tapes, and weighing the target before and after the deposition) showed that only 10% of the material is collected in a typical run. This indicates that the actual profile is broader than the assumed Gaussian, or that some of the material is not collected on the substrate. Simultaneous, parallel tape passes through the deposition zone would obviously increase the collection efficiency.

Long-term source stability tests showed that repeated firing (>500 000 pulses) in 10 mTorr of oxygen led to missing pulses (i.e. triggered pulses that resulted in no discharge to the target). However, when operating in 7–15 mTorr of nitrogen, the source performs satisfactorily, with over 10 million pulses fired without error to date. All experiments were performed with a source voltage of 16 kV and a repetition rate of 10 Hz.

The targets used for this study were made by ball-milling the desired ratios of powders of Y_2O_3, YF_3, BaF_2, and CuO, pressing 25.4 mm diameter pellets at 70 MPa, and sintering for several hours in air at 800–900 °C.

3. Composition control

An initial series of experiments was performed in which a target with Y:Ba:Cu-ratio of 1:2:3 was used and films were deposited at different pressures. The chemical composition of the deposits was then analysed by inductively coupled plasma-mass spectroscopy (ICP-MS, Thermo Jarrell Ash Corp—IRIS Med. Bench Top).

As is seen in figure 3, the correct ratio of Ba:Y = 2 is achieved at a nitrogen pressure of about 11 mTorr; however, at that pressure the deposit is copper deficient. The correct copper stoichiometry is obtained at $p = 6$ mTorr. Therefore, the correct stoichiometry cannot be obtained from a stoichiometric $(YF_3) + (BaF_2)_2 + (CuO)_3$ target. However, the ratio of Y:Ba:Cu can easily be adjusted when making targets; this deviation from stoichiometry therefore does not present a serious limitation of the process.

It is important to point out that the composition of the deposit depends strongly on the substrate position with respect to the ablation plume (data not shown); the numbers discussed above were obtained on the 1 cm × 5 cm area as shown in figure 2(a), centred at the point of the highest deposition rate. This spatial distribution indicates that the different elements ablated from the target expand according to different angular profiles. It is therefore expected that the deviation from stoichiometry is more pronounced at larger target–substrate distances.

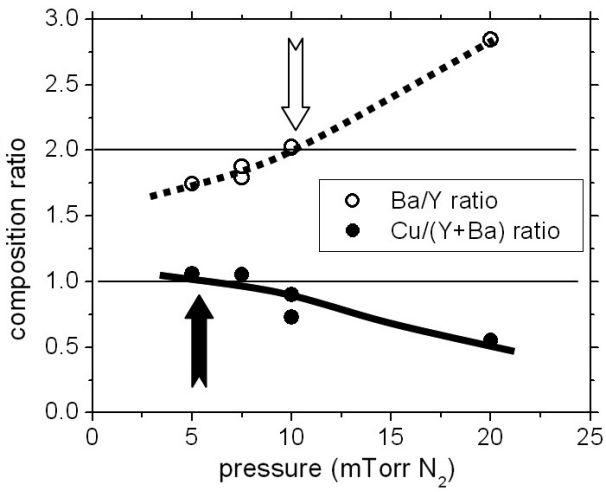

Figure 3. Composition of films deposited at various background pressures and using a target of composition $(YF_3)(BaF_2)_2(CuO)_3$.

Table 1. The dependence of film composition on deposition time (number of PED pulses at 10 Hz). Target composition: Y:Ba:Cu = 1.0:1.6:3.0.

Start (counts)	End (counts)	Composition (Y:Ba:Cu ± 0.05)
12 000	47 800	1.21:1.86:3.00
86 300	142 400	1.16:1.92:3.00
268 100	316 800	1.20:1.80:3.00

An important characteristic for the deposition of precursors onto long tapes is the stability of the process with process time. To verify that the composition of the ablated material does not change with time, we performed an experiment in which individual samples were introduced into the deposition zone at different times during a long run (316 800 pulses at 10 Hz, i.e. about 9 h). The deposits were again analysed by ICP-MS. Table 1 shows the corresponding results. A target of composition Y:Ba:Cu = 1:1.6:3 was used, resulting in slightly Y-rich and Ba-deficient films as desired. As is evident from table 1, the composition remains fairly constant.

In order to maintain consistency with the work on electron-beam evaporated precursors, a F:Ba = 2:1 ratio was desired. The fluorine content of the deposited films was determined using an Orion 96/09-combination fluoride selective electrode, with solutions obtained by dissolving the PED films in 0.5% nitric acid, followed by adding a 5.30 pH total ionic strength-adjusting buffer (TISAB). Precursors obtained from targets consisting of Y_2O_3, BaF_2, and CuO were deficient in fluorine, with F:Ba ≈ 1. For targets made of YF_3, BaF_2, and CuO, the ratio F:Ba = 2.0 ± 0.2 was obtained, and all targets used for this study were of this type.

4. Ion-probe-based diagnostics

The deposition of precursors onto lengths of tape requires long-time operation of equipment with many of the parameters held constant. It is therefore of great importance to have a method that allows the operator to continuously monitor the

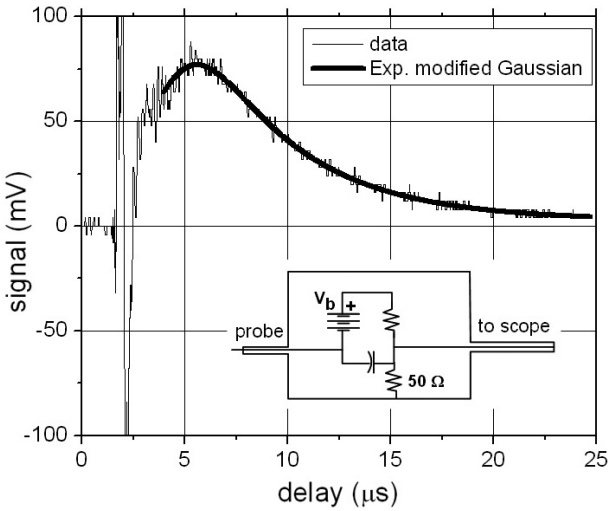

Figure 4. Ion current in the PED plume measured by a coaxial, biased ion probe, as shown schematically in the inset (bias voltage: −30 V). The measured trace (thin solid line, with the PED trigger signal defining the zero of time) can be fitted well with an exponentially modified Gaussian (thick solid line).

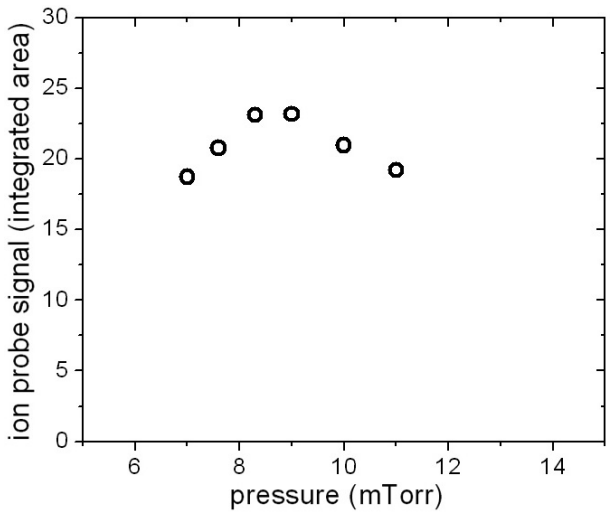

Figure 5. Integrated area of ion-probe traces (from least-square fits to an exponentially modified Gaussian curve) as a function of chamber pressure. The highest ion current is achieved at ≈9 mTorr.

key process parameters, without having to insert and remove a test sample. Ion probes have been used previously in pulsed laser deposition (PLD), as they measure the flux of ions from the target towards the substrate directly [26]. In figure 4, the inset shows the schematic of the ion-probe circuit used here. As indicated in figure 1, the probe can be inserted and removed during a deposition run, and is located close to the substrate for each measurement. Electronic noise dominates the signal during the first 3–4 μs. A positive signal then corresponds to positive ions being collected at the negatively charged exposed probe. The area under the curve is therefore proportional to the ionic charge arriving at the substrate.

The time required for the ionic species to travel from the target to the probe lets us determine an average velocity, and thus a typical kinetic energy. Due to the greatly different atomic masses of the species involved, a clear determination of this energy is impossible. Furthermore, the exact impact time of the electrons at the target is also unknown. We can safely assume, however, that the initial strong noise peak corresponds to the arrival at the probe of fast electrons ejected from the target, which occurs with only a very small delay after the impact of the primary electron pulse. Therefore, the typical velocities of the ionic species are in the range of 1 cm μs^{-1}, corresponding to kinetic energies of 10–80 eV. By comparison to earlier work on PLD diagnostics [27], we conclude that the majority of species arriving at the substrate have not collided with N_2 atoms of the background gas.

The high energy of the species impinging on the substrate points to important differences between PLD and PED. Due to the nature of the electric discharge and the requirement of a self-pinched, non-divergent electron beam, the accessible pressures are restricted to the range 4–30 mTorr. At these pressures—lower than those used in many PLD applications—thermalization of the plume with the background gas occurs only after a comparatively large path length [28]. In order to reduce the kinetic energy of the impinging species to a level more typical for PLD, the target–substrate distance in PED would therefore have to be increased if it is important to minimize plume-induced structural defects (e.g. in *in situ* film-growth applications). Due to the above-mentioned spatial variations of the deposit composition, this may not always be possible. For the non-crystalline precursor deposits studied in this work, however, plume-induced damage is not a key factor, and a short target–substrate distance can be chosen.

The area under the ion-probe curve corresponds to the total amount of species arriving at the substrate, assuming that, similarly to PLD, neutral species play a minor role, i.e. that the majority of the ions in the plasma formed by the electron ablation do not recombine with the faster—and thus spatially separated—electrons. Using an exponentially modified Gaussian to describe the curve (see figure 4), that area can readily be determined, and it is shown as a function of deposition pressure in figure 5. A well-pronounced maximum is observed at 9 mTorr, and this pressure is chosen for all subsequent experiments. Note that in our earlier work [9] we used similar pressures, based on visual inspection of the plume and on overall film quality of *in situ* deposited $YBa_2Cu_3O_{7-x}$.

As we show below, for constant deposition parameters, the deposition rate decreases with time due to target wear. It is therefore important to have a method that instantaneously determines the deposition rate at any time. For routine *in situ* monitoring during a run with the chamber pressure and target–substrate distance held constant, we show that it is sufficient to simply keep track of the peak voltage of the ion-probe signal. In fact, in a test experiment the source was operated continuously for 12 h, during which the deposition rate decreased gradually (see below). At different times during this run, a sample was placed in the deposition zone and removed again after 40 000–60 000 pulses in order to measure the actual deposition rate. The ion-probe signal was measured before and after the deposition onto the sample, and figure 6 shows the comparison of deposition rate and ion-probe peak voltage. This data clearly demonstrates that an ion probe is a

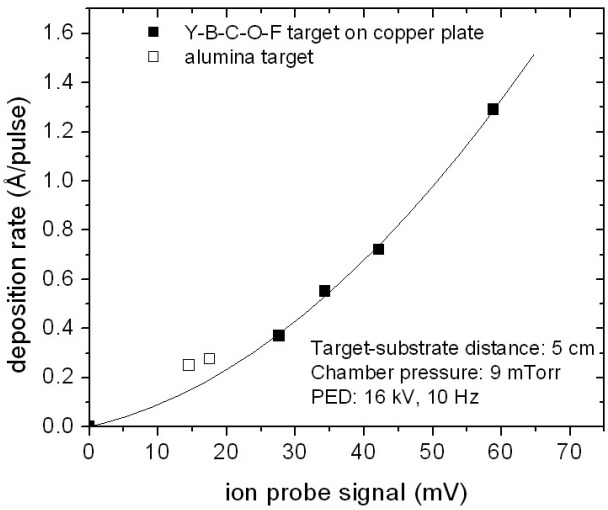

Figure 6. Correlation between deposition rate and ion-probe peak signal for two types of targets. The data points were taken at various times during a 12 h run, during which the deposition rate gradually decreased. Each data point was obtained by depositing 40 000–60 000 shots onto a sample and measuring its thickness.

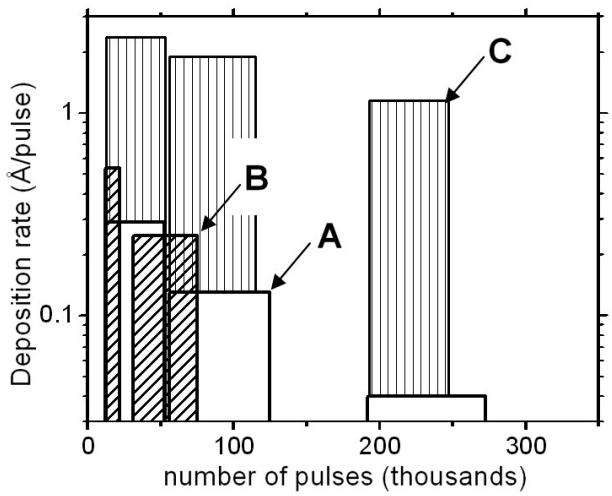

Figure 8. Deposition rate as function of process time for the target-mounting approaches shown in figure 7. The width of each rectangle corresponds to the time over which the deposition rate is averaged.

useful tool for the determination of the deposition rate during a long experiment.

5. Target wear and deposition-rate reduction

A challenging issue in PED is the observed decrease of deposition rate during prolonged runs. Due to target wear, a similar decrease is occasionally observed in PLD; however, the effects seen in PED are, under some conditions, much more severe. Contrary to PLD, where the laser beam can easily be steered across the entire target surface to obtain a more uniform usage of the material, the PED source remains fixed in space. Therefore, the rotating PED target was rastered in an oscillatory linear fashion.

One possible reason for a decrease in deposition rate is a potential change in the electron source performance with time. To test that hypothesis, two identical targets were mounted in the chamber, and we initially ablated from the first one until a visual decrease in plume intensity was observed. The targets were then exchanged *in situ*, and ablation proceeded from the second target. It was immediately observed that the plume intensity returned to the initial value, and source performance can thus be ruled out as a cause of deposition rate reduction.

Both thermal and electrical changes are possible reasons for a deterioration of the target surface, leading to a reduction in the ablation rate: the target is subject to large electrical fields, which may result in microstructure changes, and to strong thermal stresses. In fact, the target temperature may reach several 100 °C during the deposition.

A series of experiments was performed with the target mounted in different ways. Figure 7 shows the various configurations. Two methods were used to determine the deposition rate. In figure 8, we show the actually measured deposition rates on samples introduced into the plume for certain time intervals at various times. In figure 9, the results of ion-probe peak voltage measurements as a function of time are shown, allowing a more detailed observation of the time evolution. In a first experiment (configuration A of figure 7), the target was deliberately isolated thermally and electrically by placing an alumina disc between the target and its mount. Silver paste was used for all connections. As seen in figures 8 and 9, mounting the target on the alumina disc led to a very quick decrease of the deposition rate. Interestingly, replacing the alumina disc with a copper plate barely changed this behaviour B. However, when silver paste was painted onto the cylindrical sides of the target C, the deposition rate remained high for a much longer time. In a fourth configuration D, ablation took place from an alumina target. The deposition rate was low in this case for the entire experiment.

These results allow us to speculate that electrical surface conductivity (from the place where the electron pulse impinges towards the edge of the target) is a very important factor in the ablation mechanism. Removing the current path (from the edge of the target to ground) does not initially change the plume intensity (full and open circles in figure 9) but results in a very quick deterioration of the ablation process with time.

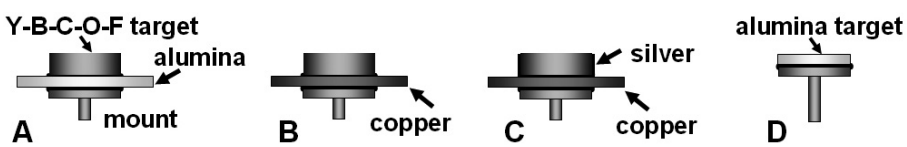

Figure 7. Various target-mounting approaches used for the study of deposition rate deterioration. A, B, and C are examples for precursor deposition, D is used to compare with a strongly insulating target.

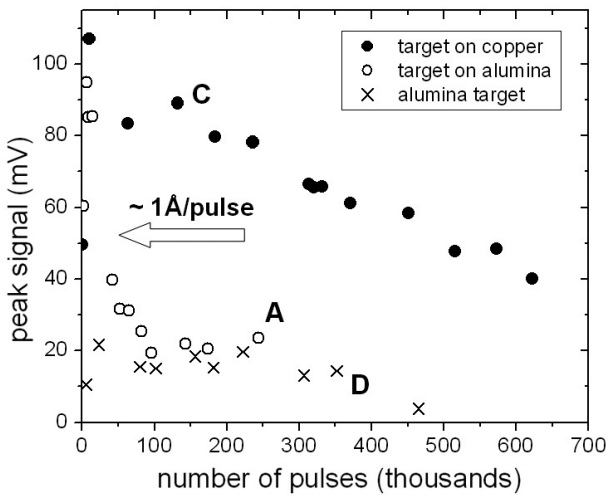

Figure 9. Ion-probe peak voltage as function of process time for the various target-mounting approaches of figure 7. Note the longer timescale than that of figure 8.

This indicates electric-field-induced changes in the target. SEM analysis and EDX-mapping across the target did not show any clear differences between well-grounded and other targets, however.

6. Application to coated conductors: $YBa_2Cu_3O_{7-x}$ on buffered Ni–W RABiTS

As an illustration of the possibilities of PED, the method has been applied to the fabrication of coated conductor tapes. 1 cm wide, buffered, rolling assisted biaxially textured substrates (RABiTS) were provided by American Superconductor Corporation (AMSC). For comparison purposes, AMSC's proprietary MOD technique for depositing 0.8 μm thick $YBa_2Cu_3O_{7-x}$ yields values of $J_c \approx 2$ MA cm^{-2} on these CeO_2/YSZ/Y_2O_3/Ni–5% W substrates. All PED depositions were carried out reel-to-reel on 30–50 cm lengths of RABiTS.

Conversion of the fluorine-based, room-temperature deposited precursor film into epitaxial $YBa_2Cu_3O_{7-x}$ occurs as the film is heated in a low partial pressure of oxygen and water. The rate of c-axis YBCO growth is, to a large part, determined by the aggressiveness of the conversion parameters [20–23]: it can be increased by increasing the water partial pressure (P_{H2O}) as well as the conversion temperature for a given oxygen partial pressure (P_{O2}).

For the reel-to-reel conversion, a 2 m long, 22-zone tube furnace incorporating seven transverse-flow modules was used as described in more detail elsewhere [22, 23] and operated at a total pressure of 1140 Torr (1.5 atm). By choosing the tape speed through the furnace and the thermal gradient along its path, the heat ramp and conversion time can be controlled accurately.

Based on the earlier results for the conversion of electron-beam co-evaporated precursors, the parameters for a slow conversion of 0.7 Å s^{-1} were chosen as follows: conversion temperature 740 °C, $P_{O2} = 120$ mTorr, P_{H2O} increasing from 4 to 30 Torr along the length of the furnace, and resident times ranging from 170 to 310 min depending on precursor thickness.

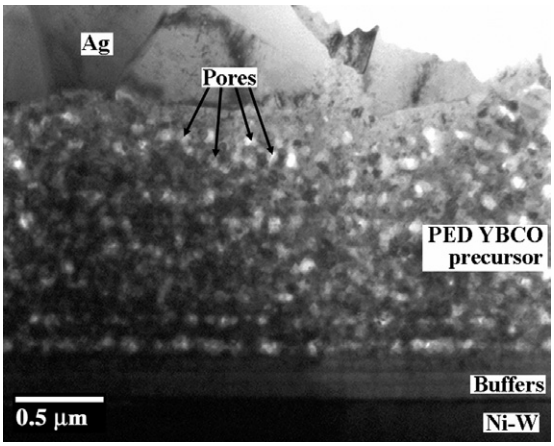

Figure 10. Cross-sectional TEM image of a quenched PED precursor after two minutes of conversion. Numerous pores of ~100 nm diameter can be seen.

Table 2. Characteristics of YBCO films of various thicknesses.

YBCO thickness (μm)	I_c (A cm^{-1})	J_c (MA cm^{-2})
0.72	117	1.6
0.86	92	1.1
0.94	100	1.1
1.30	159	1.2

With a fixed entrance temperature gradient of 31.5 °C cm^{-1}, the tape speeds corresponding to these different resident times led to ramp-up rates ranging from 15 to 27 °C min^{-1}. X-ray diffraction of the converted films showed only lines corresponding to the c-axis orientation of $YBa_2Cu_3O_{7-x}$, a $\Delta\omega$ full-width at half-maximum (FWHM) of 5.6°, and a $\Delta\phi$ FWHM of 6.8° for a 1.3 μm thick film (the corresponding values for the CeO_2 cap layer were 5.7° and 6.5°, respectively).

A significant thickness reduction of about 28% is observed during the conversion, larger than the value measured for electron-beam co-evaporated precursors. To clarify the origin of this densification, a sample was prepared similarly to the ones described above, but quenched after two minutes at the conversion temperature by removing it from the furnace onto a cold roll within about 9 s. The cross-sectional transmission electron microscopy (TEM) image shown in figure 10 clearly shows that the precursor film is porous. Similarly to MOD-deposited precursors, this porosity may possibly aid in the diffusion of H_2O into—and HF out of—the film, thereby increasing the achievable conversion rate. Corresponding results of a more rapid conversion (in excess of 7 Å s^{-1}) are described elsewhere [1].

The slowly converted superconducting samples were finally coated with 1 μm of Ag, annealed at 500 °C for 1 h and cooled at a rate of 1.5 °C min^{-1} in flowing oxygen. Critical currents were determined according to the 1 μV cm^{-1} criterion and are shown in table 2 for various thicknesses. Note that no attempt has been made to optimize the parameters for the various thicknesses, and therefore, the apparent decrease of J_c with film thickness should not be taken as an inherent property of the PED material.

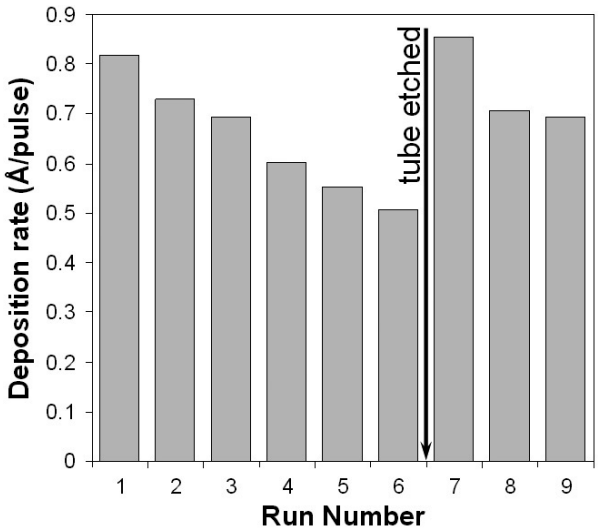

Figure 11. Average deposition rate per pulse obtained on a series of depositions (each consisting of 150 000–250 000 pulses), between which the outside of the beam tube was scraped clean. After the sixth run, the beam tube was cleaned in nitric acid.

To summarize, the results presented in this section clearly demonstrate that PED is a viable technique for obtaining coated conductors with good crystallinity and high critical currents.

7. Deposition rates and requirements for an industrial process

The system used for this study is a first implementation of a reel-to-reel tape coater, and suffers from significant drawbacks typical for a small and simple apparatus. Compared to industrial requirements, the deposition rates achieved here are low: coating a 1 m-length with 1.3 μm of precursor material (yielding 1 μm of $YBa_2Cu_3O_{7-x}$) takes approximately 10 h, corresponding to a deposition rate of 0.7 Å/pulse (averaged over the 1 cm × 5 cm deposition window).

As discussed above, the deposition rate is low at least in part because of target deterioration during a long run—initial deposition rates from a fresh target surface are typically 2 Å/pulse, more than double the averaged rate for a long run. While target wear appears to be the most significant factor leading to this deterioration, coating of the beam tube nearest to the target also plays a role. After each run, the exterior of the tube is typically scraped clean with a razor blade, leaving the interior still coated with a thin, dark layer. To determine the effect of this coating, a series of depositions was carried out in which tapes (length: 40–60 cm) were coated with a total of 150 000–250 000 pulses (the tape passed through the deposition zone 50–60 times during the deposition). After each deposition, the thickness of the film was measured, and the tube was scraped clean. After six runs, the tube was etched in nitric acid until clean, and the series was continued for three more depositions. Figure 11 shows the average deposition rate for each of these runs; clearly, a strong deterioration is observed with time, whereas etching restores the original deposition rate. This indicates the importance of a clean beam tube.

Similarly to implementations in other industrial processes [24], multiple parallel passes of the tape through the deposition zone could readily be implemented. This would easily improve the collection efficiency (and thus the deposition rate) by a factor of two. Increasing (via a source redesign) the maximum tube-to-target distance for which a stable process can be maintained (currently 2–3 mm) would reduce the amount of material deposited onto the tube, and therefore increase the deposition rate. Also, better approaches to mount and raster the target would reduce target wear; automated target exchanges will however be necessary for very long production runs. Combining a multiple-pass approach with these improvements will increase the deposition rate by a factor of four, to a rate of about 0.4 m h^{-1}.

One of the advantages of PED is the method's scalability: multiple sources—each costing a tiny fraction of excimer lasers, for example—could be mounted in series on a single tape coater, possibly increasing the production rate to 4 m h^{-1} for a ten-source system.

Finally, the repetition rate of the PED source is limited by thermal effects within the cathode and at the electrodes. Active cooling of those components would be required in order to significantly increase the repetition rate. It is clear from the above considerations that such an increase is necessary for PED to succeed as a manufacturing tool. If this can be achieved, however, deposition rates of several tens of metres per hour will be possible with a multi-source PED coater, yielding an apparatus with real applicability for industrial processes.

8. Summary and conclusions

Significant improvements to pulsed electron deposition have been implemented in this work, leading to an approach that is reliable, reproducible, and yielding high-quality coatings of complex materials in a reel-to-reel process. The parameters that control deposition rate and stoichiometry have been studied, including target composition, gas pressures, target mounting schemes, and beam tube coating. An ion probe serves as a rapid tool for the *in situ* monitoring of the process. The results also indicate that the majority of the species impinging on the substrate have not undergone collisions with the background gas and are therefore significantly more energetic than those in typical PLD applications.

Buffered, textured Ni–W alloy tapes (RABiTS) were coated at room temperature with a precursor consisting of Y, Ba, Cu, O, and F. These precursors were successfully converted into superconducting layers with critical currents $J_c = 1.6$ MA cm^{-2} (for 0.72 μm thick films), and $I_c = 159$ A cm^{-1}-width (measured on a 1.3 μm thick layer).

While there are numerous engineering challenges to be addressed (target and beam tube exchange, multiple tape passes through the deposition zone, and increasing the repetition rate of the PED source), the results presented here clearly indicate the potential of this method for an industrial process.

Acknowledgments

The authors would like to thank the American Superconductor Corporation for the supply of RABiTS. K S Harshavardhan and M Strikovski (Neocera, Inc.) are acknowledged for their continued support with the PED process. This research was sponsored by the US Department of Energy, Office

of Electricity and Energy Assurance—Superconductivity Program, under contract DE-AC05-00OR22725 with UT-Battelle, LLC, managing contractor for Oak Ridge National Laboratory.

References

[1] Lee D F, Christen H M, List F A, Heatherly L, Leonard K J, Rouleau C M, Cook S W, Martin P M, Paranthaman M and Goyal A 2005 *Physica* C submitted

[2] Jiang X L and Xu N 1989 *J. Appl. Phys.* **66** 5594

[3] Scholch H P, Fickenscher P, Redel T, Stetter M, Saemann-Ischenko G, Benker W, Hartmann W, Frank K and Christiansen J 1989 *Appl. Phys.* A **48** 397

[4] Höbel M, Geerk J, Linker G and Schultheiss C 1990 *Appl. Phys. Lett.* **56** 973

[5] Jiang Q D, Matacotta F C, Konijnenberg M C, Müller G and Schultheiss C 1994 *Thin Solid Films* **241** 100

[6] Dediu V I, Jiang Q D, Matacotta F C, Scardi P, Lazzarino M, Nieva G and Civale L 1995 *Supercond. Sci. Technol.* **8** 160

[7] Strikovski M and Harshavardhan K S 2003 *Appl. Phys. Lett.* **82** 853

[8] Choudhary R J, Ogale S B, Shinde S R, Kulkarni V N, Venkatesan T, Harshavardhan K S, Strikovski M and Hannoyer B 2004 *Appl. Phys. Lett.* **84** 1483

[9] Zhai H Y, Christen H M, Feenstra R, List F A III, Goyal A, Leonard K J, Xu Y, Christen D K, Venkataraman K and Maroni V A 2004 *Mater. Res. Soc. Symp. Proc.* **3** 21

[10] Harshavardhan K S and Strikovski M 2005 *2nd Generation HTS Conductors* ed A Goyal (Boston, MA: Kluwer–Academic) pp 108–33

[11] Iijima Y, Tanabe N, Kohno O and Ikeno Y 1992 *Appl. Phys. Lett.* **60** 769

[12] Wu W D *et al* 1995 *Appl. Phys. Lett.* **67** 2397

[13] Foltyn S R, Arendt P N, Dowden P C, DePaula R F, Groves J R, Coulter J Y, Jia A, Maley M P and Peterson D E 1999 *IEEE Trans. Appl. Supercond.* **9** 1519

[14] Usoskin A, Freyhardt H C, Issaey A, Dzick J, Knoke J, Oomen M P, Leghissa M and Neumueller H W 2003 *IEEE Trans. Appl. Supercond.* **13** 2452

[15] Iijima Y, Kakimoto K and Saitoh T 2003 *IEEE Trans. Appl. Supercond.* **13** 2466

[16] Selvamanickam V *et al* 2003 *IEEE Trans. Appl. Supercond.* **13** 2492

[17] Bauer M, Semerad R and Kinder H 1999 *IEEE Trans. Appl. Supercond.* **9** 1502

[18] Kreiskott S, Getta M, Monter B, Piel H and Pupeter N 2003 *Physica* C **383** 306

[19] Rupich M W *et al* 2003 *IEEE Trans. Appl. Supercond.* **13** 2458

[20] Izumi T, Honjo T, Tokunaga Y, Fuji H, Teranishi R, Iijima Y, Saitoh T, Nakamura Y and Shiohara Y 2003 *IEEE Trans. Appl. Supercond.* **13** 2500

[21] Lee D F, Leonard K J, Lu S W, Kroeger D M and List F A 2005 *2nd Generation HTS Conductors* ed A Goyal (Boston, MA: Kluwer–Academic) pp 149–77

[22] Paranthaman M *et al* 2000 *J. Mater. Res.* **15** 2647

[23] Lee D F *et al* 2004 *Supercond. Sci. Technol.* **17** 386

[24] Prusseit W, Nementschek R, Hoffman C, Sigl G, Lümkemann A and Kinder H 2005 *Physica* C submitted

[25] Christen H M 2005 *2nd Generation HTS Conductors* ed A Goyal (Boston, MA: Kluwer–Academic) pp 59–79

[26] Chrisey D B and Hubler G K (ed) 1994 *Pulsed Laser Deposition of Thin Films* (New York: Wiley)

[27] Lowndes D H, Geohegan D B, Puretzky A A, Norton D P and Rouleau C M 1996 *Science* **273** 898

[28] Strikovski M and Miller J H 1998 *Appl. Phys. Lett.* **73** 1733